

Twisted magnetar magnetospheres: a class of semi-analytical force-free non-rotating solutions

G. Voisin^{1†}

¹LUX, Observatoire de Paris, Université PSL, Sorbonne Université, CNRS, 92190 Meudon, France

(Received xx; revised xx; accepted xx)

Magnetospheric twists, that is magnetospheres with a toroidal component, are under scrutiny due to the key role the twist is believed to play in the behaviour of neutron stars. Notably, its dissipation is believed to power magnetar activity, and is an important element of the evolution of these stars. We exhibit a new class of twisted axi-symmetric force-free magnetospheric solutions. We solve the Grad-Shafranov equation by introducing an ansatz akin to a multipolar expansion. We obtain a hierarchical system of ordinary differential equations where lower-order multipoles source the higher-order ones. We show that analytical approximations can be obtained, and that in general solutions can be numerically computed using standard solvers. We obtain a class of solutions with a great flexibility in initial conditions, and show that a subset of these asymptotically tend to vacuum. The twist is not confined to a subset of field lines. The solutions are symmetric about the equator, with a toroidal component that can be reversed. This symmetry is supported by an equatorial current sheet. We provide a first-order approximation of a particular solution that consists in the superposition of a vacuum dipole and a toroidal magnetic field sourced by the dipole, where the toroidal component decays as $1/r^4$. As an example of strongly multipolar solution, we also exhibit cases with an additional octupole component.

Key words: key words 1, key words 2, key words 3

1. Introduction

Twisted magnetospheres of neutron stars are being investigated for the role that the twist plays in the dynamics and radiation of these stars, particularly in the case of magnetars (Thompson *et al.* 2002). By twist, it is meant that the magnetic field has a toroidal component that is supported by magnetospheric currents. Among other things, twists can affect the opacity of the magnetosphere (e.g. Viganò *et al.* 2011) because of the strong currents and particle densities they require, or affect the spin-down rate of the star by modifying the polar cap structure (Glampedakis *et al.* 2014). Untwisting is proposed to be at the origin of at least some of the stellar radiation (e.g. Beloborodov 2009; Viganò *et al.* 2011). Twists represent an energy reservoir which can provide the energy dissipated into giant magnetar flares (Mahlmann *et al.* 2019).

The equation describing an aligned non-rotating force-free magnetosphere is the Grad-Shafranov equation, and the so-called pulsar equation (Michel 1973) can be seen as its extension to rotating, relativistic, magnetospheres. A few semi-analytical solutions exist for non-rotating twisted magnetospheres (Wolfson 1995; Thompson *et al.* 2002),

† Email address for correspondence: guillaume.voisin@obspm.fr

and see Viganò *et al.* (2011) for a review. In particular, self-similar solutions have the property that both poloidal and toroidal components of the magnetic field decay with the same power-law of the radius. These solutions therefore do not asymptotically tend to vacuum. Self-similar solutions allow for multipolar-like fields (Pavan *et al.* 2009), but a single multipole is possible at a given time because the non-linearity of equations precludes linear combinations. Much work has recently been done on numerical solutions where the twist is confined, by construction, to a subset of field lines. This presents the advantage of allowing for vacuum fields outside of this region (Akgün *et al.* 2016; Ntotsikas *et al.* 2024). Some of this work has been focused on the matching of surface boundary conditions with internal solutions in order to study coupled equilibrium and evolution (Viganò *et al.* 2011; Fujisawa & Kisaka 2014; Pili *et al.* 2015; Glampedakis *et al.* 2014; Akgün *et al.* 2017). In Parfrey *et al.* (2013), it is shown that beyond a certain critical twist the force-free magnetosphere becomes tearing-mode unstable, forms a current sheet that dissipates the energy through magnetic reconnection.

In this work we present a class of semi-analytical solutions to the non-rotating Grad-Shafranov equation akin to a multipolar expansion of the magnetic field. It allows for the choice of an arbitrary set of multipoles and can asymptotically tend to a vacuum dipole. In Sec. 2 we briefly review the mathematical framework, in Sec. 3 we present the class of solutions, in Sec. 4 we present a couple of examples of solutions, and we conclude in Sec. 5.

2. Mathematical framework

For a non-rotating star, the force-free condition $\vec{j} \times \vec{B}$ (Gruzinov 2006, e.g.) leads to

$$\vec{\nabla} \times \vec{B} = \alpha \vec{B}, \quad (2.1)$$

where α is a function such that $\vec{j} = \alpha \vec{B}$ is the current density.

Taking the divergence of Eq. (2.1),

$$\vec{B} \cdot \vec{\nabla} \alpha = 0, \quad (2.2)$$

such that α is constant along a field line.

In the following we seek cylindrically-symmetric solutions, such that $\partial_\varphi = 0$ where φ is the angle around the symmetry axis. The system is therefore effectively two-dimensional, and in a system of coordinates where one of them labels magnetic field lines, Eq. (2.2) implies that α depends on that single coordinate. Because of axial symmetry the poloidal part of the magnetic field is itself divergence-free. This allows one to express it through a single Euler potential (e.g. Stern 1970) \mathcal{P} ,

$$\vec{B}_p = \vec{\nabla} \mathcal{P} \times \vec{\nabla} \varphi = \frac{\vec{\nabla} \mathcal{P} \times \vec{e}_\varphi}{rs_\theta} = \frac{r^{-1} \partial_\theta \mathcal{P} \vec{e}_r - \partial_r \mathcal{P} \vec{e}_\theta}{rs_\theta}, \quad (2.3)$$

where \mathcal{P} labels magnetic field lines †. It follows that one can write $\alpha = \alpha(\mathcal{P})$. The magnetic field reads $\vec{B} = \vec{B}_p + B_\varphi \vec{e}_\varphi$.

Expanding Eq. (2.1) in spherical coordinates, we get

$$\begin{pmatrix} \frac{1}{rs_\theta} \partial_\theta (s_\theta B_\varphi) \\ -\frac{1}{r} \partial_r (r B_\varphi) \\ \frac{1}{r} (\partial_r (r B_\theta) - \partial_\theta B_r) \end{pmatrix} = \alpha \begin{pmatrix} B_r \\ B_\theta \\ B_\varphi \end{pmatrix}. \quad (2.4)$$

† Strictly speaking poloidal field lines, but these map to general field lines through axial symmetry.

From Eq. (2.3) we see that the poloidal part of the left-hand side of Eq. (2.4) can be written

$$\begin{aligned}\frac{1}{rs_\theta}\partial_\theta(s_\theta B_\varphi) &= \alpha\frac{\partial_\theta\mathcal{P}}{r^2s_\theta}, \\ \frac{1}{r}\partial_r(rB_\varphi) &= \alpha\frac{\partial_r\mathcal{P}}{rs_\theta}.\end{aligned}\quad (2.5)$$

Since we have seen that α is a function of \mathcal{P} , we can introduce the primitive $A = \int \alpha d\mathcal{P}$, and see from Eq. (2.5) that

$$A = rs_\theta B_\varphi. \quad (2.6)$$

Inserting Eq. (2.3) into the third component of the force-free equation, Eq. (2.4), we obtain the Grad-Shafranov equation

$$-\partial_r^2\mathcal{P} - \frac{1-\mu^2}{r^2}\partial_\mu^2\mathcal{P} = \alpha(\mathcal{P})A(\mathcal{P}), \quad (2.7)$$

where $\mu \equiv \cos\theta$. Boundary conditions are such that $\mathcal{P}(\mu = \pm 1) = 0$ which ensures that the field line going out of either side of the symmetry axis is the same and avoids field-line crossings.

It is instructive to look at the example of self-similar solutions to Eq. (2.7) Low & Lou (1990); Wolfson (1995); Thompson *et al.* (2002). It consists in using the ansatz

$$\mathcal{P} = F(\mu)/r^p ; \quad \alpha(\mathcal{P}) = c\mathcal{P}^{1/p}, \quad (2.8)$$

where c is a constant, $p \geq 1$ is a constant index, and F is a function to be determined. An ordinary differential equation for F is obtained by inserting Eq. (2.8) into (2.7). This equation is non-linear and can be integrated numerically. In order to proceed, one must specify the conditions $F(\mu = 1) = \mathcal{P}(\mu = 1) = 0$ and its derivative with respect to μ , $F'(\mu = 1)$. The latter corresponds to the radial magnetic field at the pole, as can be seen from Eq. (2.3). However, the problem is thus overdetermined and the boundary condition $F(\mu = -1) = \mathcal{P}(\mu = -1) = 0$ is generally not fulfilled. For fixed c, p boundary conditions are verified for a discrete set of $F'(\mu = 1)$ which one must find numerically. Since it is physically more interesting to specify $F'(\mu = 1)$, one rather varies c , for which a discrete spectrum of solutions exist. Since Eq. (2.7) with the ansatz Eq. (2.8) is even, $\mathcal{P}(-\mu)$ is solution if $\mathcal{P}(\mu)$ is, one can integrate only until the equator at $\mu = 0$ and replace the boundary condition at -1 by $\partial_\theta\mathcal{P}(\mu = 0) = 0$ (Thompson *et al.* 2002).

3. Solutions

3.1. Ansatz

Multipolar expansions are general solutions of the vacuum electromagnetic field in spherical symmetry (Bonazzola *et al.* 2015; Pétri 2015). This motivates us to posit the ansatz

$$\mathcal{P} = B_0 R^2 \sum_{i=1} F_i(\mu) \frac{R^i}{r^i}, \quad (3.1)$$

where R is the stellar radius, B_0 gives the scale of the surface magnetic field intensity, and F_i are functions to be determined.

A heuristic for the induction of the ansatz in Eq. (2.8) consists in analysing the dependence on r on both sides of Eq. (2.7). Indeed, once one has posited the ansatz for \mathcal{P} , it is clear that the left-hand side is $\propto 1/r^{p+2}$. From this observation the form proposed for α in Eq. (2.8) appears as the simplest way to balance out the powers of

r . With the current ansatz Eq. (3.1), applying this heuristics brings us to postulate the following form for α and its integral A

$$\alpha(\mathcal{P}) = R^{-1} \sum_{i=1} (i+1) c_i \left(\frac{\mathcal{P}}{B_0 R^2} \right)^i, \quad (3.2)$$

$$A(\mathcal{P}) = B_0 R \sum_{i=1} c_i \left(\frac{\mathcal{P}}{B_0 R^2} \right)^{i+1}, \quad (3.3)$$

where c_i are a priori free coupling constants.

Keeping in mind that $[\mathcal{P}] = \text{magnetic strength} \times \text{length}^2$, it follows that the F_i are dimensionless. Similarly, from Eq. (2.1) one sees that $[\alpha] = \text{length}^{-1}$, such that the coupling constants c_i are also dimensionless. Thereafter we use units such that $B_0 = R = 1$.

3.2. Source term αA

The source term of Eq. (2.7) reads

$$\alpha A = \sum_{i,j=1} (i+1) c_i c_j \mathcal{P}^{i+j+1} = \sum_{k=3} \sum_{i=1}^{k-2} c_i c_{\underline{j}} (i+1) \mathcal{P}^k, \quad (3.4)$$

where $k = i + j + 1$ and $\underline{j} = k - i - 1$.

We formulate the powers of \mathcal{P} as a Laurent series in r ,

$$\mathcal{P}^k = \sum_{i_1, \dots, i_k} \frac{F_{i_1} \dots F_{i_k}}{r^l} \quad \text{with } l = \sum_m i_m \quad (3.5)$$

$$= \sum_{l=k} G_l^{(k)} \frac{1}{r^l} \quad (3.6)$$

$$(3.7)$$

with

$$G_l^{(k)} = \sum_{i_1 + \dots + i_k = l; i_j \geq 1} F_{i_1} \dots F_{i_k} \quad (3.8)$$

$$= \sum_{i_1=1}^{\hat{i}_1} \dots \sum_{i_{k-1}=1}^{\hat{i}_{k-1}} F_{i_1} \dots F_{i_k}, \quad (3.9)$$

where we have $\hat{i}_k = l - \sum_{j=1}^{k-1} i_j$ and $\hat{i}_j = l - \sum_{m=1}^{j-1} i_m - (k - j)$. In particular it results that $G_k^{(k)} = F_1^k$ and, more generally one can show the following functional dependence,

$$G_{k+m}^{(k)} = f(F_1, \dots, F_{m+1}). \quad (3.10)$$

This results from $\forall k, \max(\hat{i}_k) = m + 1$.

We can now decompose the source term into a Laurent series with explicit coefficients. First, inserting Eq. (3.5) into Eq. (3.4), we obtain

$$\alpha A = \sum_{k=3} \sum_{i=1}^{k-2} c_i c_{\underline{j}} (i+1) \sum_{l=k} \frac{G_l^{(k)}}{r^l}. \quad (3.11)$$

Second, we swap sums such that

$$\alpha A = \sum_{l=3} \frac{1}{r^l} \sum_{k=3}^l \sum_{i=1}^{k-2} c_i c_{\underline{j}}(i+1) G_l^{(k)} = \sum_{l=3} \frac{1}{r^l} [\alpha A]_l. \quad (3.12)$$

In order to generate the subsequent orders of the source we see from Eq. (3.12) that

$$[\alpha A]_{l+1} = [\alpha A]_l (l \rightarrow l+1) + G_{l+1}^{(l+1)} \sum_{i=1}^{l-1} c_i c_{\underline{j}}(i+1) \quad (3.13)$$

where the arrow indicates replacement of the lower indices of the G functions, and $\underline{j} = l - i$.

Here we explicit the first 5 orders of the source term,

$$[\alpha A]_3 = 2c_1^2 G_3^{(3)}, \quad (3.14)$$

$$[\alpha A]_4 = 2c_1^2 G_4^{(3)} + 5c_1 c_2 G_4^{(4)}, \quad (3.15)$$

$$[\alpha A]_5 = 2c_1^2 G_5^{(3)} + 5c_1 c_2 G_5^{(4)} + (6c_1 c_3 + 3c_2^2) G_5^{(5)}, \quad (3.16)$$

$$[\alpha A]_6 = 2c_1^2 G_6^{(3)} + 5c_1 c_2 G_6^{(4)} + (6c_1 c_3 + 3c_2^2) G_6^{(5)} + 7(c_1 c_4 + c_2 c_3) G_6^{(6)}, \quad (3.17)$$

$$[\alpha A]_7 = 2c_1^2 G_7^{(3)} + 5c_1 c_2 G_7^{(4)} + (6c_1 c_3 + 3c_2^2) G_7^{(5)} + 7(c_1 c_4 + c_2 c_3) G_7^{(6)} + [8(c_1 c_5 + c_2 c_4) + 4c_3^2] G_7^{(7)}. \quad (3.18)$$

3.3. Hierarchy

Inserting Eq. (3.12) into the Grad-Shafranov equation Eq. (2.7), and solving for each coefficient of the Laurent series in r , it transforms into a set of ordinary differential equations,

$$\forall i \geq 1, -i(i+1)F_i - (1 - \mu^2)F_i'' = [\alpha A]_{l=i+2}, \quad (3.19)$$

where by virtue of Eq. (3.10), the right-hand side only depends on $F_{j \geq i}$. As a consequence of the hierarchy of this set of equations, it can be solved iteratively up to a certain truncation order.

The boundary conditions $\mathcal{P}(\mu = \pm 1) = 0$ translate into $\forall i \geq 1, F_i(\pm 1) = 0$. In practice, we will build solutions by specifying $\{F_i'(\mu = 1)\}_{i \geq 1}$ (see below).

When all coupling constants are null, $c_i = 0$, then each element of Eq. (3.19) gives the corresponding vacuum multipole (see appendix 5): F_1 is a dipole, F_2 a quadrupole, F_3 an octupole, and so on.

If $c_1 = 0$ then all equations are linear (albeit with a potentially cumbersome source term). If the dipole order is present, that is $F_1 \neq 0$, then it is a vacuum dipole as its source term is empty. Provided that some other coupling constant is non-zero, then this dipole sources an infinity of higher-order equations. For example, if c_2 is active, then the source term of the equation for F_3 is $[\alpha A]_5 = 3c_2^2 G_5^{(5)} = 3c_2^2 F_1^5$, according to Eq. (3.16). Since all higher order terms decay with radius faster than the F_1 term, the solution is asymptotically a vacuum dipole. More generally, for $c_1 = 0$ solutions asymptotically tend to the first non-zero vacuum multipole at infinity. Since equations become linear, they can in principle be solved analytically using power series. However we here mostly use numerical integration as it appears simpler for our purposes.

On the other hand equations are highly non-linear when $c_1 \neq 0$. For example, the source term of the leading order equation for F_1 is $2c_1^2 F_1^3$ according to Eq. (3.14). As a result, these solutions do not asymptotically connect to vacuum.

3.4. Even parity and current sheet

One can see that for any solution $\{F_i(\mu)\}_{i \geq 1}$ of Eq. (3.19) on the interval $[1, 0]$, $\{F_i(-\mu)\}_{i \geq 1}$ is solution on the interval $]0, 1]$. This symmetry with respect to the equatorial plane allows us to build a solution that fulfils boundary conditions at the poles and that is defined everywhere except in that plane .

Two such solutions are in fact possible: for a given set of coupling constants $\{c_i\}_{i \geq 1}$ above the equatorial plane one can choose $\{\pm c_i\}_{i \geq 1}$ below. Indeed, the right-hand side of Eq. (3.19) depends only on products $c_i c_j$ such that a change of sign of all coupling constants has no effect. However, this changes the sign of B_φ through Eq. (2.6). We shall refer to solutions with reversed B_φ as anti-twisted solutions.

As a result, discontinuities arise at the equatorial plane for the radial and toroidal components of the magnetic field, while B_θ is continuous as can be seen from Eq. (2.3). These discontinuities are supported by a current sheet in the equatorial plane with a surface current density given by

$$\vec{\sigma} = (-2B_\phi(\mu = 0), -2B_r(\mu = 0), 0). \quad (3.20)$$

The radial current is non-zero only for anti-twisted solutions.

Odd-order vacuum solutions are even and even-order vacuum solutions are odd, as shown in appendix 5.2. A particular case of interest is when the coupling constant $c_1 = 0$. In this case equations are linear and each solution F_i is then the linear combination of a particular solution and a vacuum one. We observe that although equations are invariant under parity transformations and vacuum solutions reflect this invariance, the symmetry is broken in particular solutions independently of the value of the coupling constants. One such example is given in appendix 5 for the the third-order particular solution F_3 . It entails that particular solutions that fulfil $F_i(\mu = 1) = 0$ do not automatically fulfil $F_i(\mu = -1) = 0$ as well. This is why it is necessary to force the symmetry by introducing a current sheet which is supported by orders $F_{i \geq 3}$.

The effect on even-order multipoles is that they effectively become split multipoles. For example, a vacuum quadrupole, which is possible with the condition $c_1 = 0$, is in fact what we may call a split quadrupole. In order to keep the natural symmetry of the quadrupole, one would need to require odd parity. Unfortunately, this does not work because it introduces discontinuities in B_θ at $\mu = 0$ which are not physical since the normal component of the magnetic field must be continuous through the current sheet. Indeed, in vacuum solutions odd parity is possible because $B_\theta^v(\mu = 0) = 0$, but particular solutions generally do not fulfil that requirement.

3.5. Convergence

A necessary condition for convergence of the series defining the potential \mathcal{P} , Eq. (3.1), is that the source term αA defined by Eq. (3.12) itself converges. Indeed one expects that $F_i/r^l \sim [\alpha A]_l/r^l$ with $l = i + 2$ from Eq. (3.19). We conjecture that this is a sufficient condition in general as well, without being able to demonstrate it at this point. The special case for $c_{i \neq 2} = 0$ is discussed below and in appendix 5.

Since all equations are linear beyond first order, solutions are the sum of a particular and a vacuum solution. Vacuum solutions are proportional to the initial condition $F_i'(\mu = 1)$ (see appendix 5). Therefore, a necessary condition for convergence is that $F_i'(\mu = 1) \rightarrow_{i \rightarrow \infty} 0$. For the rest, the source term tending to zero implies the particular solutions also tending to zero.

4. Applications

In this section, we study first the simplest case that produces i) asymptotically a vacuum dipole and ii) the leading order toroidal component. Such configurations are obtained for $c_2 \neq 0$ and $c_{i \neq 2} = 0$. In all the cases presented, we present plots corresponding to the anti-twisted solutions unless otherwise mentioned. The twisted one can be straightforwardly deduced from them by symmetrising with respect to the equator, and setting the radial current-sheet component to zero, that is $\sigma_r = 0$.

We also discuss the case $c_{i \neq 1} = 0$, where the dipole order is not in vacuum, but rather interacts non-linearly. This case was already studied in previous literature but without the possibility of adding multipoles. Here we exhibit such example.

For practical purposes it is convenient to carry out the integration of Eq. (3.19) as a function of $\bar{\mu} = 1 - \mu$. In the following we denote by a dot the derivative with respect to $\bar{\mu}$, and unless otherwise stated the boundary conditions are denoted $\dot{F}_i = -F'_i(\mu = 1)$.

The `python` script used to compute the solutions and produce the figures presented in this paper is made available on the dedicated Zenodo repository [†](#).

4.1. General case with $c_{i \neq 2} = 0$

The most general solution can be expressed up to order $\mathcal{O}(1/r^5)$ as

$$\vec{B} = \vec{B}_1^v + \vec{B}_2^{v,\text{split}} \pm c_2 \frac{B_1^3 (1 - \mu^2)^{5/2}}{6 r^4} \vec{e}_\varphi + \mathcal{O}\left(\frac{1}{r^5}\right), \quad (4.1)$$

where $\vec{B}_1^v, \vec{B}_2^{v,\text{split}}$ are the vacuum dipole and split quadrupole, respectively, which we explicit in appendix 5, Eq. (5.6) and Eq. (5.9). B_1 is the dipole strength at the pole. The dipole sources a toroidal field at order $1/r^4$ through Eq. (2.6), while both vacuum fields are purely poloidal. The \pm sign in front of the toroidal term signifies the potential parity operation between hemispheres: the sign can be reversed across the equator for anti-twisted solutions. If so the solution generates a current sheet in the radial direction with surface density $\sigma_r = -2c_2 B_1^3 (1 - \mu^2)^{5/2} / r^4$, as obtained from Eq. (3.20).

In absence of split quadrupole, the twist of a magnetic field line emerging at colatitude θ is straightforward to calculate in the approximation of Eq. (4.1),

$$\Delta\varphi(\theta) = 2 \int_\theta^{\pi/2} \frac{B_\varphi}{B_\theta} \frac{d\theta'}{\sin\theta'} \quad (4.2)$$

$$= \frac{2}{3} \frac{c_2 B_1^2}{r} \left(\mu - \frac{1}{3} \mu^3 \right). \quad (4.3)$$

This is the full twist from pole to pole. In the case of the anti-twisted configuration the pole-to-pole twist is by definition 0, but the twist between a pole and the current sheet is half the above value.

At order $1/r^5$, the equation for F_3 is sourced by $3c_2 G_5^{(5)} = F_1^5$, Eq. (3.16). As shown in appendix 5, this results in a solution with discontinuous F_3' at the equator due to imposed even parity. This discontinuity is sustained by the toroidal component of the current sheet, Eq. (3.20) which therefore also decreases as $1/r^5$. Appendix 5 also gives an analytical solution of the particular solution for F_3 . Beyond this order, we consider in this paper that it is more economical to use numerical integration. Provided a quadrupole is also present, that is $F_2 \neq 0$, a toroidal field will also be present at order r^{-5} expressed by $\pm c_2 F_1^2 F_2 / r^5 \sin\theta$. More generally, none of the functions $F_{i \geq 3}$ are vacuum solutions, but instead are solutions of Eqs. (3.19) sourced by combinations of functions of lower order.

[†](#) link added upon acceptance

They are the ones that generate equatorial discontinuities supported by the toroidal component of the current sheet. In the particular case where $F_2 = 0$ and $\forall i > 1, \dot{F}_{2i} = 0$ one can show that all even-order functions are null, that is $\forall i > 1, F_{2i} = 0$.

4.1.1. Dipole

In Fig. 1 we show the anti-twisted solution sourced by a vacuum dipole. All multipoles have been computed up to order 30 and the first 10 orders are shown in Fig. 2. Since no quadrupole is present, only odd orders F_1, F_3, F_5, \dots contribute. We can see in Fig. 1 that at the surface the dipole component dominates up to a colatitude of $\sim 60^\circ$ and is dominated by higher order multipoles around the equator. The value of $c_2 = 6$ is about the highest value that we found to converge, everything else being equal. The series of F_i displays geometric convergence as can be seen in Fig. 3, as expected from the arguments given in appendix 5.

We also show in appendix 5 that in this case the problem only depends on the parameter $\rho = 3(\dot{F}_1/2)^4 c_2^2$ up to a scaling factor $\dot{F}_1/2$. This means that for a constant value of ρ , $F_i/(\dot{F}_1/2)$ are identical.

The components $F_{i>1}$ in Fig. 2 are all particular solutions, as a result of the choice of boundary condition $\dot{F}_{i>1} = 0$. Indeed, a given solution is a linear combination of a vacuum and a particular solution, $F_i = F_i^v + F_i^p$. The power-series expansion of particular solutions are proportional to $\bar{\mu}^l = (1 - \mu)^l$ where $l = i + 2$ (see appendix 5). It follows that particular solutions have derivatives equal to zero at $\mu = 1$, that is $\dot{F}_i^p = 0$. On the other hand, vacuum solutions all have a term $\mathcal{O}(\bar{\mu})$ which means that the boundary condition \dot{F}_i is entirely determined by the vacuum term.

The higher the order of F_i the more their effect is localised around the equator. This is a direct consequence of the fact that $F_i \propto \bar{\mu}^{i+2}$, which is visible in Fig. 2.

4.1.2. Dipole + octupole

In Fig. 4 we show the anti-twisted configuration of a vacuum dipole with the contribution of a vacuum octupole. We used the values $F_1' = -1, F_3' = -4c_2 = 3.2$, where c_2 has about the largest value we found that allows for convergence in this case. Figure 5 shows the components separately, and one can clearly distinguish the octupole contribution, F_3 , which slope at the origin is not null, meaning a vacuum contribution is present on top of the particular solution sourced by the dipole.

The result is a peak of the toroidal field at the surface at higher latitudes, around $\pm 45^\circ$. These contributions are however much more localised than in the dipole case above, as they result mainly from terms of the form $\propto c_2^2 F_3 F_1^2 / r^6$. This can also be seen in the very steep decay of the toroidal component of the current sheet. Beyond a few stellar radii the structure of the field tends to that of Fig. 1. The convergence plot can be seen in appendix 5.

4.2. Non-vacuum dipole + octupole

The case $c_{i \neq 1} = 0$ has already been partially studied in Low & Lou (1990). Indeed, for $\dot{F}_{i \neq 1} = 0$, it is equivalent to the self-similar model discussed in Sec. 2 for index $p = 1$, and F_1 is the only function that is not null. There is a discrete spectrum of values of c_1 for which the function is fully continuous at the equator and does not require a current sheet. For $c_1 = 0$ one has a vacuum dipole, and for higher values one has an increasing number of poles, but with a radial dependency that remains r^{-3} for all components, including the toroidal one. The difference in this work, is that it is possible to add multipoles, for example by setting $\dot{F}_3 \neq 0$. This then triggers a cascade of higher order multipoles, similarly to the above cases.

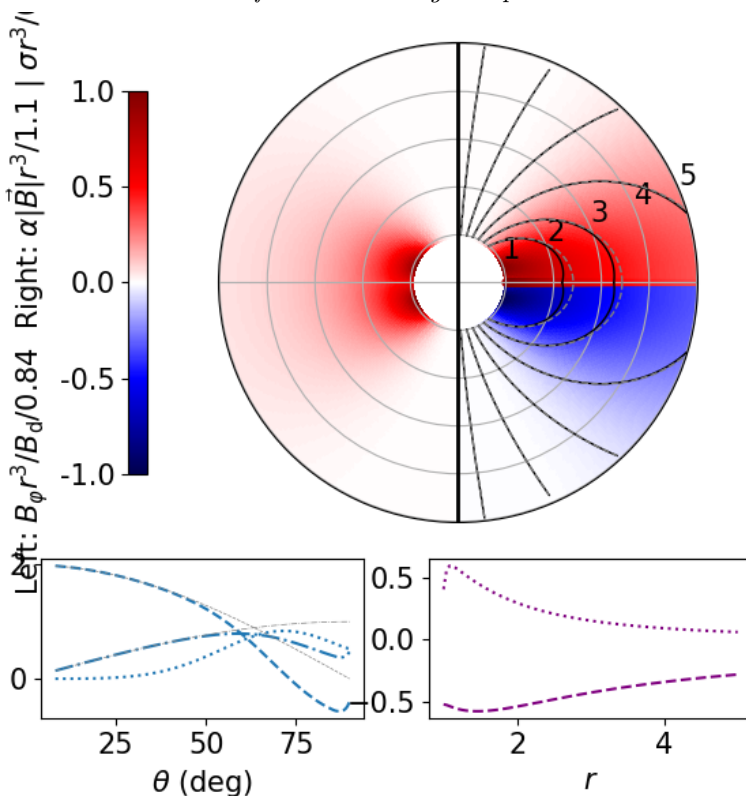


FIGURE 1. Solution for $\dot{F}_1 = B_1 = 1, c_2 = 6$ between 1 and 5 stellar radii, where B_1 is the dipole field strength at the pole. All quantities are multiplied by r^3 for better visualisation. Top left: poloidal cross-section of the current amplitude $\alpha|\vec{B}|$. The thick line on the equator represents the norm of the current in the current sheet. Top right: poloidal cross-section of the toroidal field B_φ . Poloidal magnetic field lines are shown as solid black lines, and vacuum-dipole field lines are shown for comparison as grey dashed lines. Bottom left: Magnetic-field components at the stellar surface, B_r dashed line, B_θ dot-dashed line, and B_φ dotted line in units of B_1 . For comparison, vacuum-dipole components are plotted as grey lines with corresponding styles. Bottom right: current-sheet current components σ_r , dashed line, and σ_φ , dotted line, rescaled by a factor r^3 .

This behaviour is illustrated in Figs. 6-7 where we have used $\dot{F}_1 = 1; \dot{F}_3 = 2$ at $\mu = 1$ and $c_1 = 15.981364889$, with every other initial conditions and constants equal to zero. With this particular value of the constant, F_1 is continuous at the equator and does generate a current sheet. This is why here we show the twisted case instead of the anti-twisted one. A purely toroidal current sheet is supported by the higher orders, mainly F_3 . The convergence plot is shown in appendix 5.

5. Discussion and conclusion

We present in this work a class of solutions to the Grad-Shafranov equation based on a multipolar expansion the angular part of which is determined by a hierarchy of ordinary differential equations as exhibited in Eq. (3.19). Solutions are characterised by a set of arbitrarily chosen coupling constants $\{c_i\}_{i \geq 1}$ and initial conditions for the derivatives of the angular functions $\{\dot{F}_i\}_{i \geq 1}$. The main limitation in the choice of couplings is the

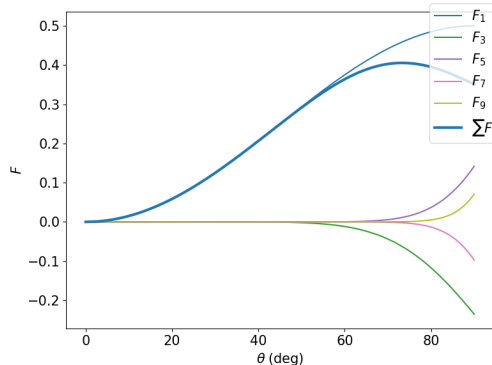


FIGURE 2. First 10 orders F_i of the solution to Eq. (3.19) for the conditions of Fig. 1. The thick blue line represents their sum up to order 30 such that it represents the potential \mathcal{P} , Eq. (3.1), on the stellar surface at $r = 1$.

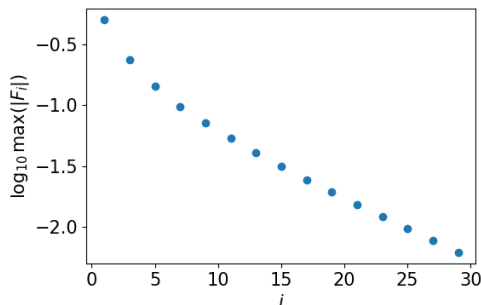


FIGURE 3. Convergence of the series defining \mathcal{P} , Eq. (3.1), for the conditions of Fig. 1. The maximum of each $|F_i(\mu)|$ for μ between 0 and 1 is plotted against its order i , where F_i is solution of Eq. (3.19). Only odd orders are shown, as even orders are all equal to 0.

necessary convergence of the series. The multipolar vacuum expansion is recovered when all coupling constants are zero.

We present a subset of solutions symmetric about the equatorial plane and supported by an equatorial current sheet. The twist, or equivalently the toroidal component of the magnetic field, can have opposite signs in opposite hemispheres.

Current sheets have been previously obtained (see in particular the numerical work of Parfrey *et al.* (2013) and references therein), and are expected to form past a certain level of twisting. Here, however, the current sheet is intrinsic to the stationary solution, albeit presumably dynamically unstable to reconnection. The case of reversed toroidal fields across the equator is reminiscent of the formation of similar internal magnetar configurations due to the Hall drift (Viganò *et al.* 2012).

A case of interest is when coupling constants are chosen such that the magnetosphere asymptotically tends to vacuum. In such case, the hierarchy of equations is linear, and can possibly be solved through power-series expansions. However the complexity of the source terms makes it rather unwieldy and one may prefer a numerical solution. To this effect, we share the `python` script used for this work (see footnote †).

We show in Eq. (4.1) the simplest solution truncated at order r^{-5} that asymptotically tends to a vacuum dipole. This results in a simple analytical expression where the leading-order toroidal component intervenes at order r^{-4} and is stronger near the equator.

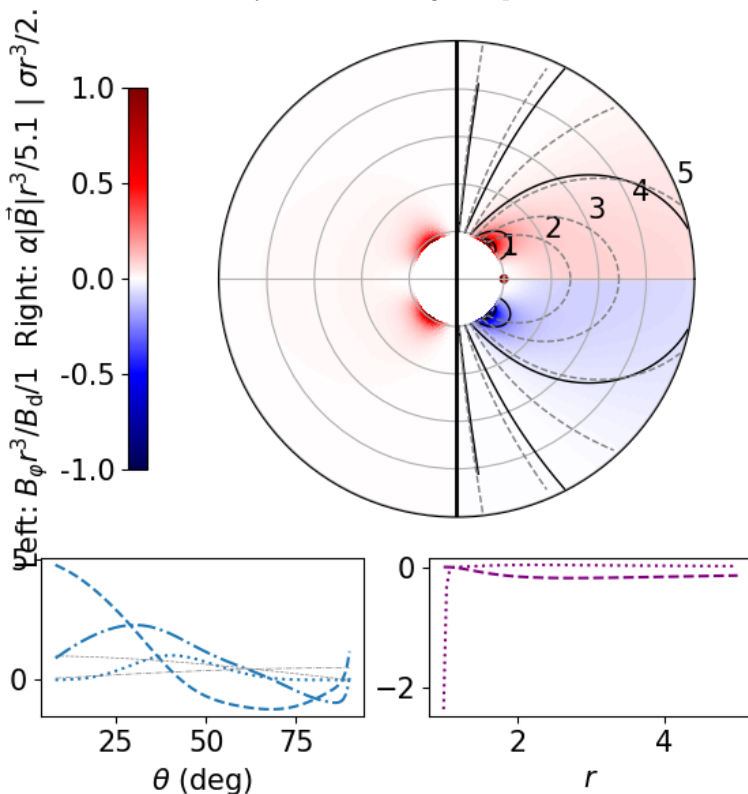


FIGURE 4. Same as Fig. 1 for $\dot{F}_1 = 1, \dot{F}_3 = 4, c_2 = 3.2$ in the anti-twisted configuration.

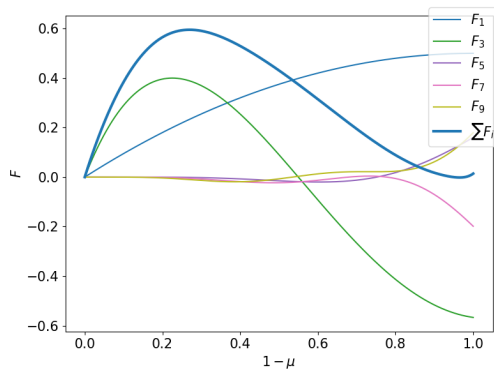


FIGURE 5. Same as Fig. 2 for the parameters of Fig. 4. The thick line shows the sum of the first 50 orders.

This class of solutions has an infinity of degrees of freedom, both in terms of coupling constants c_i and initial condition \dot{F}_i for the angular functions. Both can in principle be adjusted in order to produce a particular surface field, for example to match an internal solution. The question of whether this freedom allows one to reproduce any desired surface condition, that is the multipolar expansion forms a complete set of functions, is open. One can in principle proceed to a fit of $\{\dot{F}_i, c_i\}_{i \geq 1}$ up to a certain truncation order in order to produce the desired surface field, but this method may be technically

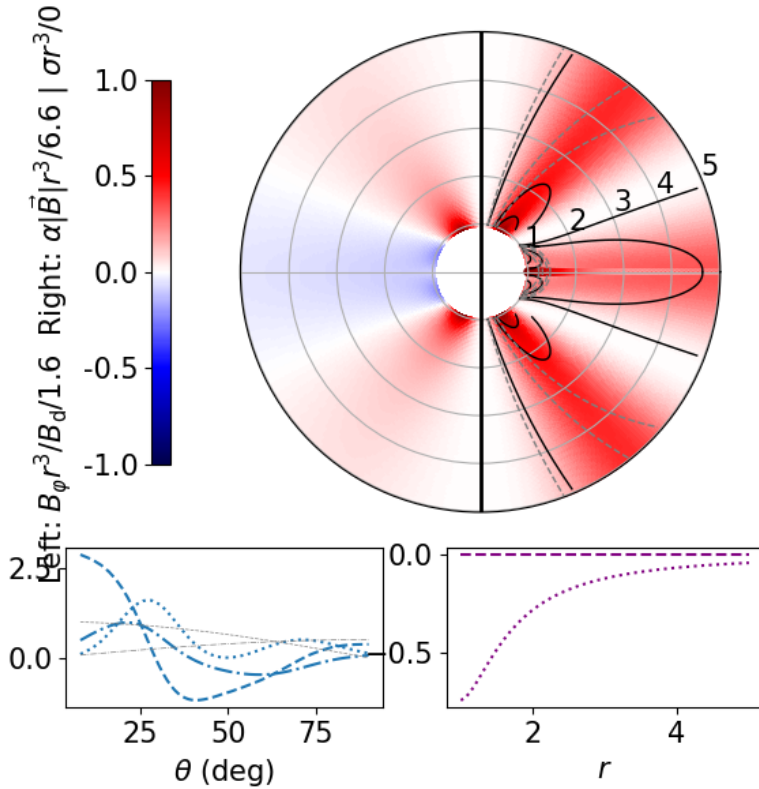


FIGURE 6. Same as Fig. 1 for $\dot{F}_1 = 1$, $\dot{F}_3 = 2$, $c_1 = 15.981364889$ and regular twist.

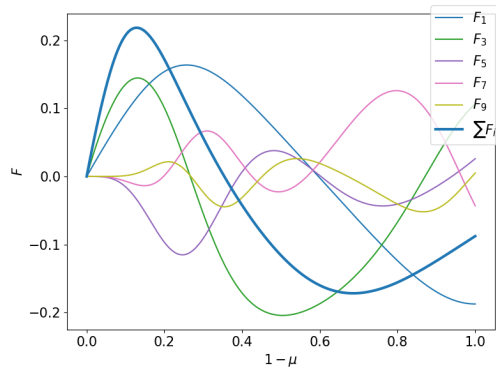


FIGURE 7. Same as Fig. 2 for the parameters of Fig. 6. The thick line shows the sum of the first 70 orders.

problematic if a large number of multipoles is required because of the large number of parameters involved. We do not exclude, however, that a more efficient method can be devised, possibly based on the hierarchical nature of the decomposition.

Acknowledgements

The author thanks Dr. Fabrice Mottez (Observatoire de Paris, CNRS) for his advice and support.

REFERENCES

- AKGÜN, T., CERDÁ-DURÁN, P., MIRALLES, J. A. & PONS, J. A. 2017 Long-term evolution of the force-free twisted magnetosphere of a magnetar. *Monthly Notices of the Royal Astronomical Society* **472**, 3914–3923, publisher: OUP ADS Bibcode: 2017MNRAS.472.3914A.
- AKGÜN, T., MIRALLES, J. A., PONS, J. A. & CERDÁ-DURÁN, P. 2016 The force-free twisted magnetosphere of a neutron star. *Monthly Notices of the Royal Astronomical Society* **462**, 1894–1909, publisher: OUP ADS Bibcode: 2016MNRAS.462.1894A.
- BELOBORODOV, A. M. 2009 Untwisting Magnetospheres of Neutron Stars. *The Astrophysical Journal* **703**, 1044–1060.
- BONAZZOLA, S., MOTTEZ, F. & HEYVAERTS, J. 2015 General solution for the vacuum electromagnetic field in the surroundings of a rotating star. *Astronomy and Astrophysics* **573**, A51.
- FUJISAWA, K. & KISAKA, S. 2014 Magnetic field configurations of a magnetar throughout its interior and exterior – core, crust and magnetosphere. *Monthly Notices of the Royal Astronomical Society* **445** (3), 2777–2793.
- GLAMPEDAKIS, K., LANDER, S. K. & ANDERSSON, N. 2014 The inside-out view on neutron-star magnetospheres. *Monthly Notices of the Royal Astronomical Society* **437**, 2–8, publisher: OUP ADS Bibcode: 2014MNRAS.437....2G.
- GRUZINOV, A. 2006 Force-Free Electrodynamics of Pulsars. *arXiv:astro-ph/0604364* ArXiv: astro-ph/0604364.
- LOW, B. C. & LOU, Y. Q. 1990 Modeling Solar Force-free Magnetic Fields. *The Astrophysical Journal* **352**, 343, publisher: IOP ADS Bibcode: 1990ApJ...352..343L.
- MAHLMANN, J. F., AKGÜN, T., PONS, J. A., ALOY, M. A. & CERDÁ-DURÁN, P. 2019 Instability of twisted magnetar magnetospheres. *Monthly Notices of the Royal Astronomical Society* **490** (4), 4858–4876, arXiv:1908.00010 [astro-ph].
- MICHEL, F. C. 1973 Rotating Magnetospheres: an Exact 3-D Solution. *The Astrophysical Journal Letters* **180**, L133.
- NTOTSIKAS, D., GOURGOULIATOS, K. N., CONTOPOULOS, I. & LANDER, S. K. 2024 Twisted magnetar magnetospheres. *Monthly Notices of the Royal Astronomical Society* **527**, 6691–6701, publisher: OUP ADS Bibcode: 2024MNRAS.527.6691N.
- PARFREY, K., BELOBORODOV, A. M. & HUI, L. 2013 Dynamics of Strongly Twisted Relativistic Magnetospheres. *The Astrophysical Journal* **774**, 92, publisher: IOP ADS Bibcode: 2013ApJ...774...92P.
- PAVAN, L., TUROLLA, R., ZANE, S. & NOBILI, L. 2009 Topology of magnetars external field - I. Axially symmetric fields. *Monthly Notices of the Royal Astronomical Society* **395**, 753–763, publisher: OUP ADS Bibcode: 2009MNRAS.395..753P.
- PÉTRI, J. 2015 Multipolar electromagnetic fields around neutron stars: exact vacuum solutions and related properties. *Monthly Notices of the Royal Astronomical Society* **450**, 714–742, aDS Bibcode: 2015MNRAS.450..714P.
- PILI, A. G., BUCCIANTINI, N. & DEL ZANNA, L. 2015 General relativistic neutron stars with twisted magnetosphere. *Monthly Notices of the Royal Astronomical Society* **447**, 2821–2835, publisher: OUP ADS Bibcode: 2015MNRAS.447.2821P.
- STERN, D. P. 1970 Euler Potentials. *American Journal of Physics* **38** (4), 494–501, publisher: American Association of Physics Teachers.
- THOMPSON, C., LYUTIKOV, M. & KULKARNI, S. R. 2002 Electrodynamics of Magnetars: Implications for the Persistent X-Ray Emission and Spin-down of the Soft Gamma Repeaters and Anomalous X-Ray Pulsars. *The Astrophysical Journal* **574** (1), 332, publisher: IOP Publishing.
- VIGANÒ, D., PONS, J. A. & MIRALLES, J. A. 2011 Force-free twisted magnetospheres of neutron stars. *Astronomy & Astrophysics* **533**, A125, publisher: EDP Sciences.

VIGANÒ, D., PONS, J. A. & MIRALLES, J. A. 2012 A new code for the Hall-driven magnetic evolution of neutron stars. *Computer Physics Communications* **183**, 2042–2053, aDS Bibcode: 2012CoPhC.183.2042V.

WOLFSON, R. 1995 Shear-induced Opening of the Coronal Magnetic Field. *The Astrophysical Journal* **443**, 810, aDS Bibcode: 1995ApJ...443..810W.

Appendix

Vacuum solutions

Vacuum solutions to the Grad-Shafranov equation are usually expressed using Legendre polynomials (see e.g. Viganò *et al.* 2011). For the purpose of this work we find it insightful to outline a demonstration of these solutions and explicit the first multipoles.

In vacuum Eq. (3.19) becomes,

$$\forall i \geq 1, -l(l+1)F_l^v - (1-\mu^2)F_l^{v''} = 0. \quad (5.1)$$

We remark that this could directly have been obtained from the Grad-Shafranov equation, Eq. (2.7), with an ansatz of the form $\mathcal{P} = F_l^v(\mu)/r^l$.

Since we specify boundary conditions at $\mu = 1$, we will seek a power-series solution of the form $F_l^v = \sum_{i=0} a_i \bar{\mu}^i$, where $\bar{\mu} = 1 - \mu$. Indeed, expansions around $\mu = 0$ do not always converge at $\mu = 1$. Injecting this series into (5.1), one finds after a few manipulations that solutions to the equations follow the sequence defined by

$$\forall i > 0, a_{i+1} = a_i \frac{i(i-1) - l(l+1)}{2i(i+1)}, \quad (5.2)$$

and $a_0 = 0$. This sequence is initialised by choosing a_1 . One sees that $a_{i>l+1} = 0$, such that these solutions are finite polynomials. Since $a_0 = 0$, these solutions satisfy $F_l^v(\bar{\mu} = 0) = 0$, as required. It is less obvious what their behaviour is at $\bar{\mu} = 2$ ($\mu = -1$). A change of variable $\bar{\mu} \rightarrow 1 - \mu$ shows that these solutions are even for odd values of l and odd for even values, meaning that $F_l^v(\mu = \pm 1) = 0$, and all required boundary conditions are matched. It is immediate to see that $a_1 = -F^{v'}(\mu = 1) = \dot{F}^v(\bar{\mu} = 0)$ where the dot denotes differentiation with respect to $\bar{\mu}$.

These solutions form a multipole basis. We explicit the first orders,

$$F_1^v = a_1 \left(\bar{\mu} - \frac{1}{2} \bar{\mu}^2 \right) = \frac{a_1}{2} (1 - \mu^2), \quad (5.3)$$

$$F_2^v = a_1 \bar{\mu} \left(1 - \frac{3}{2} \bar{\mu} + \frac{1}{2} \bar{\mu}^2 \right) = \frac{a_1}{2} \mu (1 - \mu^2), \quad (5.4)$$

$$\begin{aligned} F_3^v &= a_1 \bar{\mu} \left(1 - 3\bar{\mu} + \frac{5}{2} \bar{\mu}^2 - \frac{5}{8} \bar{\mu}^3 \right) \\ &= -\frac{a_1}{8} (1 - 6\mu^2 + 5\mu^4), \end{aligned} \quad (5.5)$$

Using Eq. (2.3) with $\mathcal{P} = F_l/r^l$, we obtain expressions for the vacuum magnetic fields,

$$\vec{B}_1^v = \frac{B_1}{r^3} \left(\cos \theta \vec{e}_r + \frac{\sin \theta}{2} \vec{e}_\theta \right), \quad (5.6)$$

$$\vec{B}_2^v = \frac{B_2}{r^4} \left((2 \cos \theta - 1) \vec{e}_r - \cos \theta \sin \theta \vec{e}_\theta \right), \quad (5.7)$$

$$\vec{B}_3^v = \frac{B_3}{r^5} \left(\left(\frac{5}{2} \cos^4 \theta - \frac{3}{2} \cos \theta \right) \vec{e}_r + \left(\frac{\sin^3 \theta}{8} \theta - \frac{\sin \theta}{2} \right) \vec{e}_\theta \right), \quad (5.8)$$

where B_1, B_2, B_3 are the magnetic strengths at the pole corresponding respectively to $a_1, a_1/2, a_1$ in the notations of Eqs. (5.3)-(5.5)

In the case of imposed even parity across the equator, the quadrupole field becomes a split quadrupole which can be written

$$\vec{B}_2^{\text{v,split}} = (H(\mu) - H(-\mu)) \vec{B}_2^{\text{v}}, \quad (5.9)$$

where $H(x)$ is the Heaviside step function such that $H(x \geq 0) = 1$ and $H(x < 0) = 0$.

Example of analytical solution for F_3

We consider the case where F_1 is a vacuum dipole, Eq. (5.3), $F_2 = 0$ and c_2 is the only non-zero coupling constant. In this case, the source term of the F_3 equation in Eq. (2.7) is $[\alpha A]_5 = 3c_2^2 G_5^{(5)} = 3c_2^2 F_1^5$ as can be seen from Eq. (3.16).

We solve the equation for $\phi_3 = F_3/(3c_2^2 \dot{F}_1(0)^5)$ where we denote \dot{F} the derivative of F with respect to $\bar{\mu} = 1 - \mu$,

$$-12\phi_3 - \bar{\mu}(2 - \bar{\mu})\ddot{\phi}_3 = \left(\bar{\mu} - \frac{1}{2}\bar{\mu}^2\right)^5. \quad (5.1)$$

In order to get a particular solution $\phi_3^{(p)}$ we proceed exactly as for the vacuum solutions of Sec. 5, by expanding $\phi_3^{(p)} = \sum_{i=0} \alpha_i \bar{\mu}^i$, obtaining

$$\sum_{i=0} \bar{\mu}^i [-2(i-1)i\alpha_{i+1} - \alpha_i(l(l+1) - i(i-1))] = \left(\bar{\mu} - \frac{1}{2}\bar{\mu}^2\right)^5, \quad (5.2)$$

where here $l = 3$.

We find the particular solution

$$\begin{aligned} \phi_3^{(p)} = & -\frac{8}{15}\bar{\mu}^6 + \frac{88}{105}\bar{\mu}^7 - \frac{24}{49}\bar{\mu}^8 + \frac{113}{882}\bar{\mu}^9 - \frac{17}{1323}\bar{\mu}^{10} \\ & - \frac{1}{97020}\bar{\mu}^{11} + \sum_{i=12}^{\infty} \alpha_i \bar{\mu}^i \end{aligned} \quad (5.3)$$

where the polynomial part results from matching the first 11 terms with the source term on the right-hand side of Eq. (5.1), and the series is generated by using the relation in Eq. (5.2) (replacing a with α) for $i \geq 11$ seeded with $\alpha_{11} = 1/97020$. The terms up to order $\mathcal{O}(\bar{\mu}^5)$ do not appear here because they correspond to the vacuum solution in Eq. (5.1). The full solution is thus $F_3 = F_3^{\text{v}} + 3c_2^2 \dot{F}_1(0)^5 \phi_3^{(p)}$ where the first term is given by Eq. (5.1) and the second one by Eq. (5.3). We have checked that Eq. (5.3) matches the numerical integration used in the main text within numerical error.

We see that the particular solution of Eq. (5.3) fulfils the boundary condition $\phi_3^{(p)}(\bar{\mu} = 0) = 0$ and that its first derivative is equally null $\dot{\phi}_3^{(p)}(\bar{\mu} = 0) = 0$, meaning that the slope at the origin is entirely given by the vacuum solution. More generally, It can be shown by induction that the source terms of the equation of order i are proportional to $\bar{\mu}^l(1 + \mathcal{O}(\bar{\mu}))$, with $l = i + 2$, implying that $\phi_i^{(p)} = \mathcal{O}(\bar{\mu}^l)$.

On the other hand, this solution is neither symmetric with respect to $\mu = 0$ nor does it fulfil the second boundary condition $\phi_3^{(p)}(\bar{\mu} = 2) = 0$. Indeed, we find numerically $\phi_3^{(p)}(\bar{\mu} = 2) \simeq 0.057$. As a consequence, in order to respect the boundary conditions we construct a solution by forcing a symmetry with respect to the equator. In particular, this implies a discontinuity of \vec{F}_3 at the equator, which results in a discontinuity of the radial magnetic field supported by a toroidal current sheet (see main text).

The series term in Eq. (5.3) converges for $\bar{\mu} \leq 2$, however its derivative is not defined at $\bar{\mu} = 2$ as its series diverges. Indeed one can show that at $\bar{\mu} = 2$ the series is asymptotically given by $\alpha_i \bar{\mu}^i \sim 1/i^2$, the derivative of which is $\sim 1/i$ and thus diverges. From a practical point of view, we note that the polynomial part of Eq. (5.3) is accurate to $\sim 10^{-5}$, which we expect to be sufficient for most applications.

Convergence

5.1. Discussion of the $c_{i \neq 2}$ case

A case of interest that we exhibit in Sec. 4 is when $c_{i \neq 2} = 0$, $F_1 \neq 0$, and $F_{i > 1} = 0$. That is, we have a vacuum dipole which sources higher multipoles through the coupling c_2 . Only functions $\{F_{2i+1}\}_{i \geq 1}$ are non zero, and the fact that $F'_{2i+1} = 0$ means that all solutions are particular solutions without vacuum terms (see main text and appendix 5). We show below that the right-hand side of Eq. (3.19) is, up to a factor of order 1, $[\alpha A]_{l=i+2} \propto \beta_i = \rho^i F'_1/2$ for $i \geq 3$, where $\rho = 3(F'_1/2)^4 c_2^2$. In addition, we show that dividing both sides of each equation in Eq. (3.19) by $F'_1/2$ results in F_i/F'_1 depending only on ρ .

We call $\chi_i = F_i/(F'_1/2)$ and get for the first orders,

$$\mathcal{L}_1 \chi_1 = 0 \quad (5.1)$$

$$\mathcal{L}_3 \chi_3 = \rho \chi_1^5 \quad (5.2)$$

$$\mathcal{L}_5 \chi_5 = \rho n_1 \chi_3 \chi_1^4 = \mathcal{O}(\rho^2) \quad (5.3)$$

$$\mathcal{L}_7 \chi_7 = \rho(n_2 \chi_5 \chi_1^4 + n_3 \chi_3^2 \chi_1^3) = \mathcal{O}(\rho^3) \quad (5.4)$$

where $\mathcal{L}_i = -i(i+1) - (1-\mu^2)\partial_{\mu^2}^2$ is the linear operator on the left-hand side of Eq. (3.19). The n_i are the number of terms involved that can be calculated from Eq. (3.8), but they are irrelevant for our current discussion.

By definition $\chi_1 \sim 1$. Indeed it is a vacuum solution, Eq. (5.3), such that $\max(|\chi_1|) = 1$. It follows that $\chi_3 \sim \rho$, $\chi_5 \sim \rho^2$ up to a factor of order 1. The fact that particular solutions of χ_i are proportional to the amplitude of the right-hand side is immediately apparent by looking for series solutions as we do in appendix 5.

We proceed by induction to show that $\chi_{2i+1} \sim \rho^i$. Initialisation has just been shown, therefore we assume that this is true for all functions up to order $2i+1$. At order $2i+3$, we see from Eq. (3.8) that the right-hand side is

$$\rho G_{l+2}^{(5)} = \sum_{i_1 + \dots + i_5 = l+2; i_j \geq 1} \chi_{i_1} \dots \chi_{i_5}, \quad (5.5)$$

with $l = 2i+1+2$. We see that the only combinations of i_1, i_2, i_3, i_4, i_5 possible can be obtained by taking those present at order l in $G_l^{(5)}$ and by replacing a single i_j by i_j+2 . In these terms the largest i_j is $2i-1$ for the term $\chi_{2i-1} \chi_1^4$. Since $\chi_{i_j+2} \sim \rho \chi_{i_j}$, these terms are indeed of order $\mathcal{O}(\rho^{i+1})$. Thus the induction is proven.

Based on this argument, we expect that the χ_{2i+1} can be bounded by a geometric sequence with common ratio $\sim \rho$. Convergence then corresponds to $\rho \lesssim 1$, which means $|c_2| \lesssim 2.3 F'_1(1)^2$. Numerically, we observe approximate geometric convergence up to $|c_2| \lesssim 6 F'_1(1)^2$. It is to be noted, that we have here neglected the increasing number of terms on the right-hand side. However one can see by looking at Eq. (3.8) that, without detailed calculation, this number can be bounded by l^4 . Thus the number of terms increases polynomially, which does not affect geometric convergence.

The series that actually must converge is χ_i/r^l . It follows that if $\chi_{2i+1} = \mathcal{O}(\rho^i)$ then

$\chi_i/r^l = \mathcal{O}((\rho/r)^i)$. As a result, if the series converges at the surface, for $r = 1$, then it converges for any $r \geq 1$. If $\rho = \rho_{\max}$, the largest value for which convergence is allowed at $r = 1$, then the series is expected to diverge for $r < 1$. This is the behaviour we numerically observe.

5.2. Supplementary convergence plots

In Figs. 8 - 9 we exhibit the convergence of the dipole+octupole and non-vacuum dipole + octupole cases, respectively.

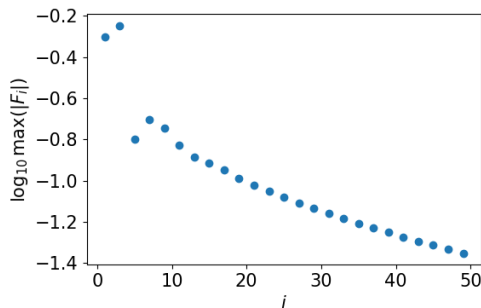


FIGURE 8. Similar to Fig. 3 for the parameters of Fig. 4.

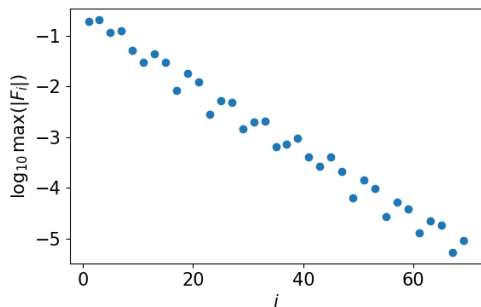


FIGURE 9. Similar to Fig. 3 for the parameters of Fig. 6.

Parity

We want to show that the source terms of even-order functions F_{2i} are odd and even for odd-order functions F_{2i-1} in the case $c_{i \neq 2} = 0$. The source term of the equation for F_i is $3c_2^2 G_{i+2}^{(5)}$ for $i \geq 3$ as can be seen from Eq. (3.13). For $i = 3$, $G_5^{(5)} = F_1^5$ is even, as desired. For $i = 4$, $G_6^{(5)} \propto F_2 F_1^4$, which is odd, equally as desired. Equation (3.8) shows that $G_l^{(5)} = \sum_{i_1, \dots, i_5} F_{i_1} \dots F_{i_5}$ with $i_1 + \dots + i_5 = l$ and $l = i + 2$. From Eq. (3.10), we know that $G_l^{(5)}$ depends only of function $F_{j < i}$, such that we can prove by induction the result. Given $i > 2$, we assume that parity properties are fulfilled for all $j < i$. Then, for any $l > 4$, if l is even then an even number of odd indices is required which means that the number of even indices is odd. It follows that $G_l^{(5)}$ is odd for even l , as desired.

Conversely, for odd l we need an odd number of odd indices and an even number of even indices, such that $G_l^{(5)}$ is even, as desired. Thus, we have proven the result.